X-ray-edge problem in metals. I. Universal scaling in alkali-alkali alloys

T.-H. Chiu,* Doon Gibbs,† J. E. Cunningham, and C. P. Flynn
Department of Physics and the Materials Research Laboratory, University of Illinois at Urbana-Champaign, Urbana, Illinois 61801
(Received 30 November 1984)

We report outer-core excitation spectra of alkali-alkali alloys. The results are obtained by differential reflectance methods using synchrotron radiation on quench-condensed samples. Striking changes of line shape take place with changing composition. All available threshold profiles for alkali-metal alloys and pure metals conform to a universal scaling relationship defined by parameters related to the electronic structure of the excited configuration. The sharp "x-ray edges" with an overshoot at threshold occur only when the excited alkali-metal-atom valence orbitals localize at or below the band bottom and other atoms of the same type neighboring the active core in the Periodic Table. A linear absorption profile rising from zero absorption at threshold is observed when the excited orbitals mix strongly with conduction-band states.

I. INTRODUCTION

In this research we investigate the "x-ray-edge" problem of metals and alloys. The present paper, referred to as I, reports core-excitation spectra and presents analysis for samples made by alloying together two different alkali metals. Paper II, which follows immediately, describes studies of foreign alkali-metal atoms adsorbed on the surfaces of alkali-metal host metals. The composite work thus focuses on the way in which the core-excitation spectrum of an alkali-metal atom is modified by an alkali-metal conduction-electron liquid, to which it can be coupled in different ways.

Previous work has largely concerned excitations of the pure metals. The $np^6(n+1)s \rightarrow np^5(n+1)s^2$ excitation spectra of the pure alkali metals Na ($n=2$), K ($n=3$), Rg ($n=4$), and Cs ($n=5$) exhibit certain similar characteristics. Each has a sharp leading edge with an overshoot or spike at threshold, as seen in Fig. 1, due to Ishii *et al.*[1] These effects have been described by a famous theory originating in ideas of Anderson[2] and Mahan,[3] and reaching completion in treatments by Nozières and de Dominicis[4] for optical excitations, and by Doniach and Šunjić[5] for photoemission processes when treated in the "sudden" approximation. The theory has been reviewed recently by Wilkins.[6] Together with the $L_{2,3}$ edges of Mg and Al,[7] the alkali-metal spectra have provided the testing ground through which these Mahan—Nozières—de Dominicis (MND) theories have been linked to experiment. A burst of activity terminating some five years ago led to experiments on optical excitation, x-ray photoemission, luminescence, electron inelastic scattering, and total-electron-yield spectroscopy of these systems.[6–8] It is established that the Li-metal $1s^22s \rightarrow 1s2s^2$ excitation threshold differs from the remaining alkali-metal outer-core excitations by a much larger rounding. This arises from coupling to vibrational excitations, among other possible causes.[9] For the remaining alkali metals, together with Mg and Al, it appears that the theoretical expressions can possibly provide at least a semiquantitative fit to much of the data. Wide and unresolved differences of opinion remain about the degree to which the theory offers a predictive description of experiment. Detailed accounts of some chosen examples, together with elaborate data fitting, are given in Refs. 7 and 8.

Alloys offer controlled experiments by which the effects of coupling core excitations to the conduction-electron liquid can be explored. These bear directly on the theory also, since the MND results apply, in principle, to

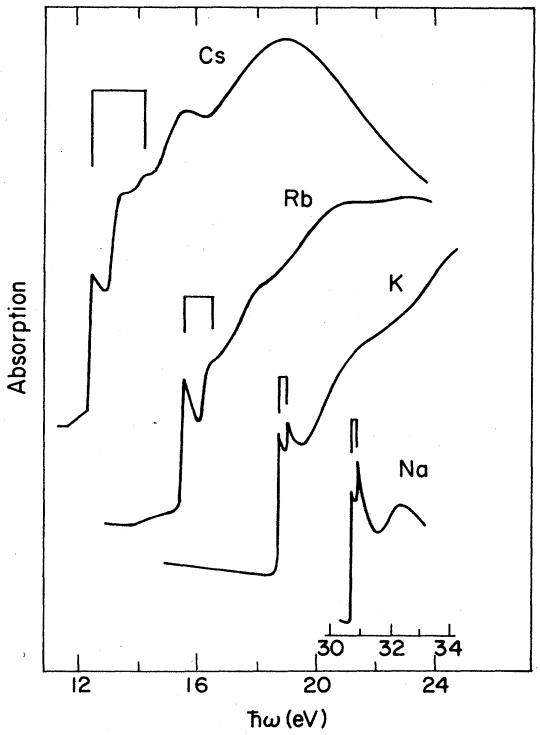

FIG. 1. Outer-core excitation spectra of Na, K, Rb and Cs, according to Ishii *et al.* (Ref. 1). Brackets indicate features thought to be spin-orbit partners.

host and impurity excitations alike. Only the *changes* of conduction-electron phase shift caused by the local excitation enter into the theoretical results.[4] Previously, experiments on impurities have revealed qualitative dependences of excitation profile on impurity properties. Like the alkali-metal host spectra in Fig. 1, the $p \rightarrow s$ outer-core spectra of rare-gas[10] impurities and halogen impurities[11] each exhibit a characteristic threshold behavior which, however, differs widely from the one chemical type to the next. Recent work has shown for halogen and rare-gas atoms that adsorbates coupled to the metal surface have spectra rather similar to those of the same impurities coupled to the bulk metal.[12] Predictions obtained using the MND prescription for bulk impurities are quite different from even the qualitative experimental trends. There is apparently a strong dependence of the excitation spectra on local electronic structure which the theory does not treat correctly.

The work described in papers I and II was undertaken with the results for rare-gas and halogen impurities coupled to alkali-metal hosts in mind. These impurities represent a large local perturbation on the metal. It is natural to inquire how similar systems behave when the perturbation is much weaker; alkali-metal impurities then appear as attractive candidates for investigation. In addition, alkali-alkali alloys are the simplest of materials from a theoretical standpoint, with just one conduction electron per atom. These factors led Miyahara *et al.* to the first studies of core excitations in alkali-alkali alloys.[13] Their work employed only the heavy alkali metals, for which small changes of threshold energy and line shape on alloying were observed. A wider variety of alloys has been covered in the present systematic investigation using samples (both alloy and adsorbate systems) prepared by quench condensation at liquid-He temperatures. Major, qualitative changes of alkali-metal core-excitation characteristics are observed to take place when the composition is varied. The changes are comparable with the differences between rare-gas impurity and alkali-metal host spectra. These results are reported in paper II for adsorbed alkali-metal atoms and in the present paper for alloys.

As the alloy ground state is a simple metal with one electron per cell, the large observed effects on the excitation spectrum focus attention on the electronic structure of the excited *local* configuration. It turns out that no complete studies of the excited-state structure exist because the MND theory requires phase shifts only for electrons at the Fermi level. Upon consideration it becomes apparent that important changes of electronic structure do occur in the alkali-metal-atom excited configuration. In particular, the $(n+1)s^2$ orbitals of the core-excited alkali-metal atoms certainly decouple from the host conduction band in the pure metals as states *bound at or below the band bottom.* Such phenomena are well known in x-ray spectroscopy to cause sharp structure in the form of "white lines" at the threshold of core excitations.[14] These facts bring into open consideration the question of whether or not existing interpretations of the x-ray-edge phenomena are completely mistaken. The experiments we report appear to establish that sharp "x-ray-edge" thresholds with an overshoot occur when bound valence states are present in the excited configuration and other atoms of the same species neighbor the excited core. Brief reports of these results have appeared elsewhere.[15]

The work is presented as follows. Studies of adsorbates and surface impurity layers are described in paper II.[16] The equipment is also described there, with only enough mentioned in paper I to make the paper self-contained. Section II of paper I provides a semiempirical description of the alkali-metal-atom excitation process using the "$Z+1$ model" to predict alkali-metal-atom core-excitation energies with an accuracy on the order of 0.1 eV. Also given in Sec. II is a description of electronic structure in the alkali-metal-atom excited configuration, including the important question of bound-state formation. Section III then presents the experimental results for loys, together with necessary experimental details. In the Discussion, Sec. IV, we show how the present alloy results, those of Miyahara *et al.*,[13] together with data for the pure alkali metals, all conform, at least approximately, to a universal scaling behavior in terms of parameters defined by the description of excited-state structure in Sec. II. The paper ends with a brief Summary, Sec. V.

II. THRESHOLD ENERGIES AND ELECTRONIC STRUCTURE

Our purpose in this section is to analyze the threshold energies at which the outer-core transitions occur in the pure alkali metals. We shall use empirical methods based on the "$Z+1$ approximation" in order to remove from the discussion the uncertainties of actual electronic structure calculations.[17] In favorable cases this empirical procedure is able to reproduce core-excitation thresholds correctly to ~ 0.1 eV. Comparable accuracy is not yet forthcoming from electronic structure calculations for core levels, although cluster methods have been used to obtain similar accuracy for shallow excitations.[18]

The $Z+1$ model is described elsewhere in detail. Suppose atom A undergoes a core excitation to A^* in a solid-state environment. Figure 2 shows how the *atomic* ground and excited states suffer cohesion shifts E and E^* as they are accommodated in the solid, so that the excitation threshold, given by the difference of *total* energies between the two configurations, is

$$\hbar\omega = \hbar\omega_a + E - E^* , \tag{1}$$

with $\hbar\omega_a$ the excitation energy of the free atom. The special point of the $Z+1$ model is that the lowest core-excited state of an atom is chemically similar to the ground state of its right-hand neighbor in the Periodic Table. Thus Cs* $5p^5 6s^2$ and Ba $5p^6 6s^2$ have identical $6s^2$ valence structures surrounding small positive cores, and their ionization energies to the $[6s^1]^+$ configuration are almost the same at 4.89 and 5.21 eV, respectively.[19] Even this small difference is reduced when the alkali-metal-atom value is averaged over spin orientations. This near identity of the valence structures means that the energy change E^* as A^* is accommodated in the solid can be modeled by the analogous chemical behavior of the element neighboring it in the Periodic Table. In what fol-

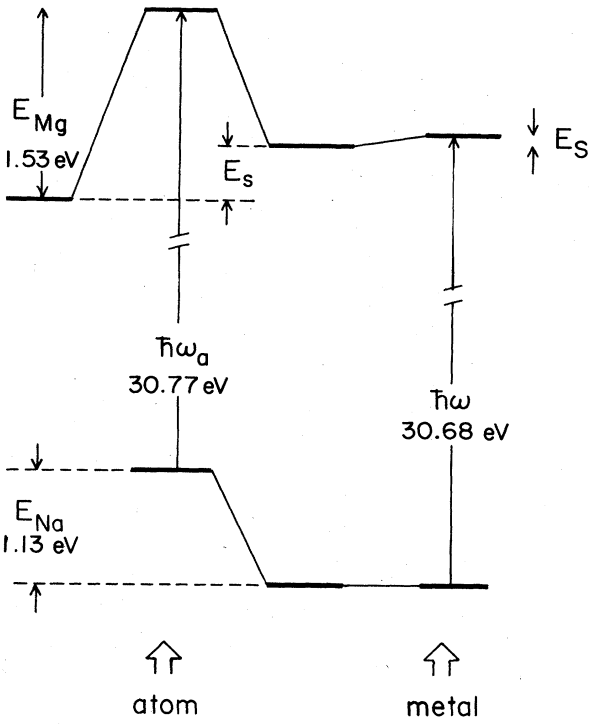

FIG. 2. Sketch modeling the energy threshold of the $2p^6 3s \rightarrow 2p^5 3s^2$ excitation of Na in Na metal. The cohesive energy E_{Na} is released when the ground state is dissolved in the metal. The analogous total-energy change of the excited configuration, $\hbar\omega_a$ above in the atom, is obtained using the $Z+1$ approximation from properties of Mg in Na metal. The cohesion shift is broken into the Mg cohesive energy E_{Mg} and the energy E_s needed to dissolve Mg in Na metal. A small Stokes shift, E_S, arising from lattice distortion, is added. E_{Na} and $E_{\mathrm{Mg}}-E_s$ are the specific values of E and E^* of the $Z+1$ model for this particular example.

lows we first apply these ideas to the core excitations of host and impurity centers in the alkali metals.

A. Pure alkali metals

Figure 2 is adapted specifically to our purpose here as an illustration of the Na $3p$ threshold in sodium metal. When the ground state of Na is placed in the metal it releases exactly the cohesive energy $E=E_{\mathrm{Na}}$. Experiments show[22] that the $2p^6 3s \rightarrow 2p^5 3s^2$ excitation energy of the atom is $\hbar\omega_a = 30.77$ eV. The excited $2p^5 3s^2$ configuration is modeled chemically by Mg $2p^6 3s^2$. The energy release when Mg is accommodated in the metal may be represented by two terms: first the cohesive energy[20] of pure Mg, E_{Mg}, and second the (negative of the) energy of solution, E_s, required to transfer a Mg atom from Mg to Na (by convention E_s is positive when energy must be supplied to effect the transfer). To model the optical transition a final small correction is needed. This is the Stokes shift E_S, to correct for the lattice relaxation which occurs in the alloy but not in the optical excitation. Then the core-excitation threshold in the solid occurs at

$$\hbar\omega = \hbar\omega_a + E_{\mathrm{Na}} - E_{\mathrm{Mg}} + E_s + E_S \ . \tag{2}$$

Approximate expressions for the shift E_S are directly available from the results given by Flynn[21] using the $Z+1$ approximation.

Values of the atomic excitation energies, cohesive energies, and Stokes shifts relevant to the alkali-metal-atom core excitation in pure alkali metals are collected in Table I. Unfortunately, the energies E_s of solution are not generally available, and so Table I is organized to display

$$\hbar\omega - E_s = \hbar\omega_a + E_Z - E_{Z+1} + E_S \ , \tag{3}$$

and the energies of solution are deduced from the difference of the observed and calculated excitation energies, namely $E_s' = \hbar\omega_{\mathrm{obs}} - (\hbar\omega - E_s)$, with $\hbar\omega_{\mathrm{obs}}$ the observed threshold energy. As the penultimate column of Table I makes evident, these deduced energies of solution are very consistently about 0.4 eV. Experimental values of E_s may be estimated from available data in the form of observed solubilities c only for two cases. These solubilities[24] are 0.23 at. % for Be in Li metal at 1005 K and about 2 at. % for Mg in Na metal at 913 K. The value quoted for Na in the last column of Table I is $E_s = -kT \ln c$, which gives about 0.3_4 eV for Na (and about 0.5_3 eV for the analogous Li result). These are values derived for the liquid, rather than for the solid, assuming that the dilute alloy equilibriates with the pure metal.

There is excellent consistency between the observed E_s

TABLE I. Energies (in eV) of alkali-metal-atom $np^6(n+1)s \rightarrow np^5(n+1)s^2$ excitations in atom, $\hbar\omega_a$, and in metal, $\hbar\omega$, and cohesive energies E_Z of alkali metals and E_{Z+1} of their alkaline-earth neighbors, and the Stokes shifts E_S of solid-state excitations. A comparison of $\hbar\omega_a$ with $\hbar\omega - E_s$, as calculated from Eq. (3), gives deduced energies of solution E_s' for comparison with measured values E_s (last two columns), where available.

Z	$\hbar\omega_a$	$\hbar\omega$	E_Z	E_{Z+1}	E_S	$\hbar\omega - E_s$	E_s'	E_s
Na	30.77[a]	30.68[c]	1.13	1.53	0.04	30.41	0.36	0.3_4[e]
K	18.71[b]	18.27[d]	0.94	1.83	0.06	17.88	0.39	
Rb	15.31[b]	14.92[d]	0.88	1.71	0.05	14.53	0.39	
Cs	12.30[b]	11.75[d]	0.83	1.86	0.07	11.34	0.41	

[a]Reference 22.
[b]Reference 19.
[c]Reference 23.
[d]Reference 1.
[e]Reference 24.

from solubility data for Na (and Li) and the values E_s' deduced from the excitation energies. The empirical procedure eliminates core-specific parts of the total energies and leaves the chemical features apparent, with a rather small energy uncertainty. Given the solubility data, of course, the $Z+1$ model permits the core-excitation energies to be simulated with this same precision, as has been found in other applications also.[17]

B. Alkali-metal impurity spectra

Much the same methods may be employed to predict the core-excitation thresholds of alkali-metal atoms as impurities. A comprehensive tabulation is once more prevented by the unavailability of some required alloy data, but enough exist for clear patterns to emerge. The impurity case differs from Fig. 2 only in that the energy shift E of the ground configuration now contains an energy of solution of the impurity in the given host, in addition to the cohesive energy of the pure impurity. Thus, we must now interpret E_s in Eq. (2) as the *difference* between the energies of solution A^* and A exhibit in that solvent.

A comprehensive investigation has shown that the heats of intersolution among the heavy (liquid) alkali metals are all very small,[25] 0.1 eV or less. No data are available for heavy alkaline earths in the heavy alkali metals. Size factors are not, however, likely to be important and the values probably remain close to 0.4 eV as in Table II. Therefore the excitations of Cs, Rb, and K as impurities in each others host lattice are expected to have thresholds close to those observed in the pure metals.

The situation is rather different for light alkali host metals because the heavy alkali metals exhibit high energies of solution in Li and Na.[24] For example, Cs dissolves in Li only to the extent of 0.01% at 1033 K, whereas the alkaline earths in Li exhibit the following solubilities: Be, 0.23 at.% at 1005 K; Mg, soluble to 30 at.%; Ca, 0.43 at.% at 414 K, Sr, 2 at.% at 407 K; Ba, <1 at.% in the solid. With Cs *less* soluble than the alkaline earths, E_s in Eq. (2) becomes negative, whereas in pure Cs it is positive and of size 0.3 eV (Table I). This leads directly to the expectation that the Cs excitation threshold in Li may be red-shifted from its value in pure Cs by $\gtrsim 0.3$ eV. The experimental confirmation of this shift is reported below.

TABLE II. Energies (in eV) of ionization for alkali-metal-atom p^6s configurations, I, and for p^5s^2 excited configurations, I^* deduced from data in Ref. 19. Also given are cohesive energies E_c and Fermi energies E_F. Free-electron values of E_F are given for the heavy alkali metals and "measured" values for Na and Li (free-electron values in parentheses). These data lead to the results of Figs. 3 and 12, showing how bound-state formation affects the core-excitation profile.

	I	I^*	E_c	E_F
Li	5.39	9.32	1.66	3.7 (4.74)
Na	5.14	7.21	1.13	2.5 (3.24)
K	4.34	5.77	0.94	2.12
Rb	4.18	5.40	0.88	1.85
Cs	3.89	4.89	0.83	1.59

C. One-electron energies

In addition to the dependence on the total configurational energies discussed above, we shall find that the core-excitation profiles in alkali-metal alloys are sensitive to the electronic structure within the excited configuration. The relationship between host band states and the excited valence levels of the excited center is of particular interest. It is therefore helpful to understand chemical trends in the electronic structure. A brief analysis of these factors is provided in what follows.

The most important point is that the $(n+1)s$ levels of the core-excited alkali-metal atoms in their $np^5(n+1)s^2$ configurations are more deeply bound that in the $np^6(n+1)s$ ground states. Table II documents this by values of the ionization energies I and I^* of the ground and excited states, respectively, obtained from Ref. 19. The difference between I^* and I is significant for each metal when compared to the conduction-band width. Figure 3 shows the conduction-band states and the excited $(n+1)s^2$ levels on the same energy scale for each of the alkali metals. The conduction bands in the figure are placed on an appropriate scale of absolute energy by drawing in bands with free-electron widths, starting from Fermi energies at the free-atom ionization energies I (this reproduces the alkali-metal cohesive energies as $2E_F/5$ quite well). The $(n+1)s^2$ levels are introduced by assuming that the local electron-hole interaction is the same in the metal as in the atom. The excited levels are then drawn in place, lowered by the atomic value of the splitting, from the band mean at $3E_F/5$. The purpose of Fig. 3 is to show whether or not degenerate mixing is likely to occur between conduction-band orbitals and the valence levels of the excited alkali metal. Rather different considerations, involving screening, etc., would be needed if other phenomena, related, for example, to charge transfer, were of concern instead.

As we point out elsewhere,[15] the construction in Fig. 3

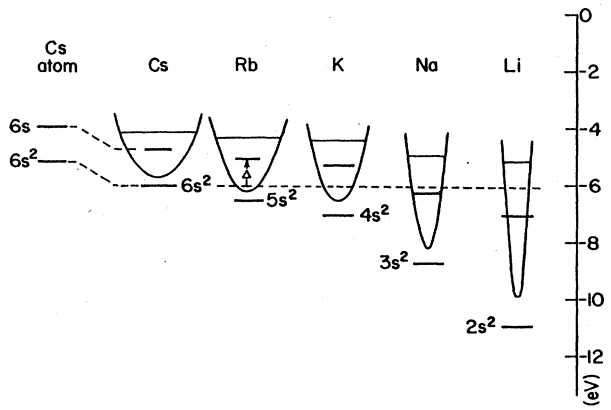

FIG. 3. Diagram showing the absolute location of s^2 levels of the excited alkali-metal atoms with respect to the alkali-metal conduction bands, drawn here with free-electron widths. In each metal the excited core levels localize below the band bottom as bound states. The horizontal dashed line indicates the tendency of the Cs $6s^2$ levels to mix degenerately with the conduction-band orbitals of the lighter alkali metals.

indicates that the excited host valence orbitals fall below the band bottom as bound states for each of the pure alkali metals. The splittings scale with the bandwidths to maintain very similar excited-state structures in the various alkali metals. Undoubtedly this arises from the same general balance between Coulombic and kinetic energy which determines the alkali-metal lattice spacings and hence their bandwidths in the first place. Since bound-state formation can profoundly affect excitation line shapes, this is an important new issue which warrants a central place in the extensive literature on alkali-metal-atom "x-ray edges."

The chemical forces apparent in Fig. 3 may be modified by solid-state effects, so that the final electronic structures possibly differ from those shown. One may ask, for example, whether or not the atomic electron-hole interaction is screened by band states, and the splitting thereby reduced. It is important also to recognize that a clear distinction between bound and propagating orbitals exists only in one-electron theories.[26] No reliable calculations of electronic structure exist for the alkali-metal excited configurations. Careful studies have, however, been made for Mg in Li metal and Be in Li metal by very different methods. In the $Z+1$ approximation these serve as models of excited Na in Li metal and excited Li in Li metal, respectively. The results of these calculations are therefore of direct consequence here.

Ingelsfield[27] has employed Green's-function methods to examine the local properties introduced by Mg impurities in Li metal. He finds that Mg causes a large peak density of states having $3s$ character at the Li band bottom. This is in very satisfactory agreement with the location of the Na* $3s^2$ levels in Fig. 3, together with the band-bottom location of Li also given there.

Both the Mg and Be ground states in Li metal have been treated by Boisvert *et al.*[18,28] using cluster methods with the unrestricted Hartree-Fock approximation augmented by many-body perturbation theory. The clusters were small, so the energy spacings of valence orbitals remained quite large. For Mg the $3s^2$ orbitals appeared 2.7 eV above the lowest band orbital, whereas for Be the $2s^2$ and band orbitals become strongly admixed, with the lowest combination occurring 2.0 eV below the normal band-bottom state. These results are once more in satisfactory general accord with the chemical trends obtained more simply by the methods of Fig. 3.

By way of summary we note that the available detailed calculations do not fully illuminate the question of bound-state formation in the alkali-metal excited configuration. On the other hand, they clearly establish that the chemical trend of Fig. 3 is at least qualitatively correct. In the later discussion we employ the same ideas to discuss the dependence of optical line shape on excited-state structure. Strong correlations are found between structure and optical response. It should be clearly understood that the electronic structure discussed there require future confirmation through detailed calculations. Regardless of the outcome of such calculations, however, the experimental correlations retain validity as relationships between the chemical driving forces (Fig. 3) and the consequent effect on core line shapes. The question of the precise electronic structure is somewhat secondary in this regard. The available evidence nevertheless suggests that the simple arguments leading to Fig. 3 do give at least a semiquantitatively correct description of the excited-state electronic structure. It is established beyond question, for example, that a marked tendency to bound-state formation is present in the alkali-metal excited state.

III. EXPERIMENTS AND RESULTS

A. Experimental methods

In earlier work we report measurements made on rare-gas atoms adsorbed on alkali metals and other related systems by techniques similar to those employed here.[29] In the present research, the basic method involves differential reflection of *s*-polarized synchrotron-radiation light from pure and doped samples. Monochromatized light from the University of Wisconsin Tantalus II light source was chopped alternately between two parallel paths which reflect from the two samples. Both source and detector drifts are eliminated from the fractional difference when the two beams are monitored by a common detector. In practice, the two samples were thin metal films on two adjacent areas of the same optically flat sapphire substrate.

The samples were quench-condensed onto the substrate *in situ* at liquid-He temperature from atomic beams monitored by carefully calibrated quartz-crystal oscillators. The use of ultrahigh vacuum and liquid-He temperatures inhibits both sample contamination and thermal evolution to nonrandom configurations. Spectra presented here are characteristic of random, probably microcrystalline, alloys. Mg or Al was first deposited from an evaporation boat onto the sapphire substrate to promote high and featureless reflectivity through the energy range of interest, and was then covered by the alkali-metal sample. The sources employed for alkali-metal evaporations are described in paper II. Belljar vacuums in the low-10^{-10}-Torr range were invariably achieved, aided by cryopumping from the Cu can at liquid-He temperature surrounding the sample. Pressures inside the can were undoubtedly much lower, for the same reason. No changes of spectral profile originating from surface contamination were observed.

It has been established in other work[29] that differential reflectance measurements of this type give spectra rather accurately proportional to the imaginary (absorptive) part of the thin-film optical response. This holds for the present work with the following restriction. Time limitations on use of the synchrotron beamline mandated that several successive samples be fabricated on the same substrate, each serving as substrate for the next. In a few cases, a noticeable spectral distortion occurred as layers of high optical density built up and modified the featureless reflectivity of the underlying substrate metal. Invariably this distortion left the systematics of the profile clearly discernible, but with spectral differences reduced through the regions of high optical density. Results in which such distortions occur are identified by the symbol (*S*), indicating optical saturation, in what follows.

For efficient operation, the thickness and concentration of samples had to be carefully balanced to provide substantial but not excessive absorption from each film. Details of the 28 alloy layers investigated in this work are collected in Table III.

B. Results

The data reported below pertain to excitations of K, Rb, and Cs cores. The Na $2p$ excitation is not well adapted to the present technique because the substrate reflectance is too low above 30 eV. Also, the Li excitation has a different symmetry, as mentioned above, and is therefore not of related interest. We investigated only those systems for which the core excitation under examination occurred at lower energy than that of the second alkali-metal component. This avoided cases of high optical density and still allowed measurements to be made in the interesting regime of impurity dilution. Our work includes the seven systems Cs*-Li, Cs*-Na, Cs*-K, Rb*-Li, Rb*-Na, K*-Li, and K*-Na. In addition, Miyahara *et al.*[13] have studied K*-Cs, K*-Rb, and Rb*-K, thereby providing 10 alloy systems in all for which results are available. The superscript asterisk is used here to indicate the atom with the optically active core.

In what follows the data are grouped and discussed by the sequence of cores Cs, Rb, and K investigated. All spectra are shown normalized, which involves scaling the actual results linearly to amplitudes appropriate for a surface coverage of 10^{16} cm^{-2} of the cores under investigation, in place of the actual surface density. This facilitates the comparison of line shape and integrated oscillator strength among successive spectra taken with differing compositions.

1. Cs in Cs-Li, Cs-Na, and Cs-K

In the free atom, the principal $5p^6 6s \rightarrow 5p^6 s^2$ transitions of Cs occur[19] at 12.30 eV ($P_{3/2}$) and 13.52 eV ($P_{1/2}$). The O_3 absorption edge in the pure solid occurs just below 11.8 eV with a width of about 60 meV. The $5p$ absorption of Cs in Li, Na, and in K determined in the present research is shown in Figs. 4, 5, and 6 respectively. The Li results appear particularly good, although some slight saturation occurred for the runs at 85 and 74 at.% Cs. These data will be described first.

The top curve in Fig. 4 was taken with a coverage of 2.8×10^{15} cm^{-2} or perhaps 6 monolayers of Cs deposited on Li metal. This closely resembles spectra for pure Cs (Fig. 1) in the sharp threshold edge and small overshoot, but is doubtless distorted somewhat by the Cs-Li and Cs-vacuum interfaces. When Li is added to form a Cs-Li alloy, the edge broadens into a Lorentzian shape on which the cusp remains weakly visible. Only after the peak vanishes at 64 at.% Cs can a realistic separation of the profile into spin-orbit partners be made (dashed lines) with an assumed splitting of 1 eV, close to that of the free atom. Here and for higher Li additions the long Lorentzian tail has disappeared, leaving a Gaussian-like profile. As the Cs dilute limit is reached, with the alloys at 5.2 and 3.7 at.% Cs, the profile near threshold appears noticeably linear with some rounding (see inset). This latter interpretation requires a linear threshold beginning at about 11.3 eV, red-shifted by 0.4_5 eV from that of pure Li at 11.7_5 eV, and with a rounding over perhaps 0.2 eV. These two principal features of the dilute system are consistent with the red shift predicted by the $Z+1$ model (see Sec. II B) and with the typical magnitude of vibrational broadening expected in these alloys.[21]

Very similar phenomena are observed in the Cs-Na sys-

TABLE III. Thickness t (Å) and concentration c (at. %) of the alkali-alkali alloys investigated in this research.

Core:	Cs			Rb		K	
Alloy:	Cs-Li	Cs-Na	Cs-K	Rb-Li	Rb-Na	K-Li	K-Na
c (at. %)	85	85	50	66	52	76	6.6
t (Å)	28	70	45	16	15	21	210
c	74	65	20	61	7.5	41	3.6
t	18	50	60	15	75	26	210
c	64	45	6	40		8.4	
t	18	35	150	20		83	
c	50	4.0		3.5		1.6	
t	20	210		120		120	
c	39	1.0					
t	28	310					
c	23						
t	36						
c	5.2						
t	130						
c	3.7						
t	140						

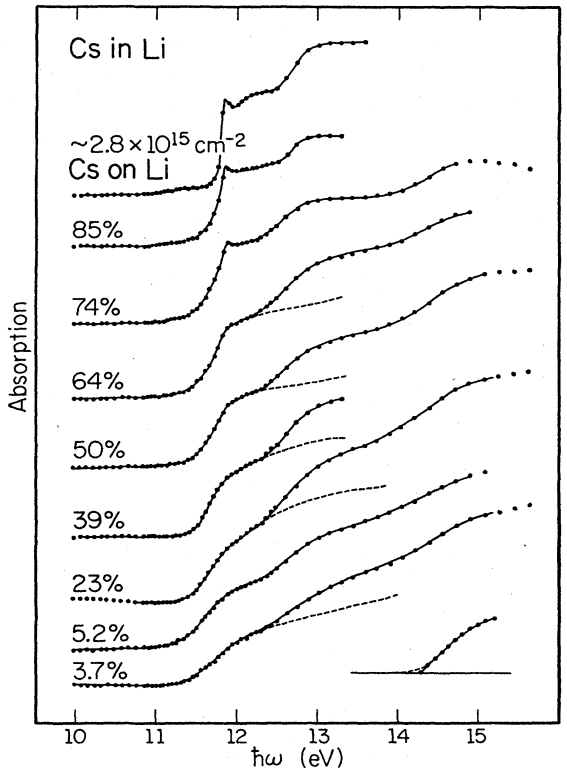

FIG. 4. Absorption spectra of Cs in Cs-Li alloys of various compositions (at. %). All curves are scaled to a coverage of 10^{15} cm^{-2} for convenient comparison. Dashed lines indicate spin-orbit decomposition of $P_{3/2}$ and $P_{1/2}$ components with ratio 2:1, in cases where this can be effected smoothly. The top curve, for about 6 monolayers of Cs on Li metal, shows the approximate profile for pure Cs. Inset is a phonon-broadened linear threshold profile for comparison with the linear spectra obtained for the Cs dilute limit.

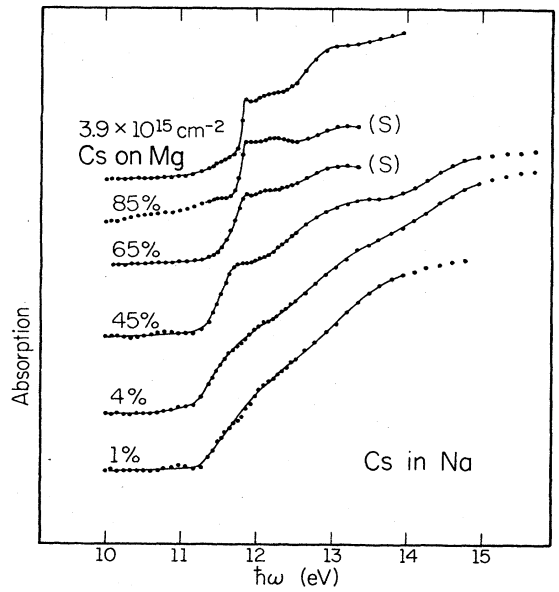

FIG. 5. Absorption spectra of Cs in Cs-Na alloys of various compositions (at. %) scaled as in Fig. 4. The top curve is for about 8 monolayers of Cs on Mg metal, showing the pure Cs edge on top of the underlying profile of Cs on Mg metal (see paper II for details). The symbol (*S*) marks data that are distorted at high optical density.

tem. A spectrum for 3.9×10^{15} cm^{-2} Cs on Mg is shown with the Cs*-Na results in Fig. 5. The sharp edge and overshoot resemble the Cs spectrum in Fig. 4, but an additional weak sloping feature extends from the edge down to about 11.2 eV. In paper II it will become clear that this part of the response originates from Cs atoms in contact with Mg and is not relevant to the present discussion. The results for 85 and 65 at. % Cs in Na are, unfortunately, both partly saturated, but the progressive broadening of the sharp edge and the persistence of the overshoot both remain visible. By 65 at. % the surface-induced feature has disappeared and the Lorentzian spread of the profile above threshold is evident. In the Cs dilute limit at 4 and 1 at. % Cs the spectrum becomes linearlike, just as for Cs-Li, and it becomes possible to make a smooth spin-orbit separation using reasonable values for the splitting.

For Cs in K, the spectra, shown in Fig. 6, differ markedly from those for the Li and Na host alkali metals; they agree with the general features reported by Miyahara *et al.*[13] for this same system. Although the overshoot is not visible for 50 at. % K and above, the core-excitation edge in our spectra remains fairly abrupt down to 6 at. % Cs, and very weakly red-shifted from the edge of pure Cs. It is probable that these characteristics hold down to infinite dilution. Note that the Mg-induced linear component underlying the edge for Cs on Mg (Fig. 5) appears to persist across the phase diagram, as also does the small structure immediately above the edge, near the 12.3-eV excitation energy of the Cs atom. We have no explanation for these phenomena at present.

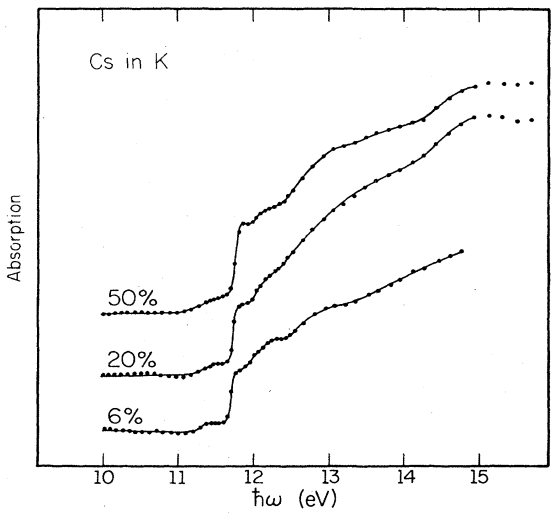

FIG. 6. Spectra of Cs in Cs-K alloys of various compositions (at. %) scaled as in Fig. 4 (see Figs. 4 and 5 for pure Cs). The threshold is shifted and broadened only slightly. The weak structure below the abrupt edge is of unknown origin.

2. *Rb in Rb-Li and Rb-Na*

Rb has its principal $4p^6 5s \rightarrow 4p^5 5s^2$ core excitations at 15.31 eV ($P_{3/2}$) and 16.16 eV ($P_{1/2}$) in the free atom.[19] In the pure solid the sharp N_3 edge occurs at 14.9 eV.[13] Our data in Figs. 7 and 8 for excitation of the Rb $4p^6$ core are generally less satisfactory than the results for Cs and K core excitations. Nevertheless, they clearly reveal the edge broadening which is of principal interest here.

Figure 7 shows two runs for alloys with 52 and 7.5 at. % Rb in Na and two spectra for pure Rb on Na taken at coverages near 5 and 3 monolayers. The latter show the sharp Rb edge and overshoot, followed by a rounded spin-orbit partner at higher energy, much as in the Cs spectra. At 52 at. % the edge is noticeably broadened and is further broadened and red-shifted for the 7.5-at. % alloy, near to the dilute limit.

For Rb in Li in Fig. 8, the main Rb edge is broadened by about 65 at. % Rb, but it retains a sharp peak. An attempt to separate the response into spin-orbit partners fails for much the same reasons of smoothness found earlier for Cs in Li. A progressive broadening occurs down to the dilute limit at 3.5 at. % Rb, where a reasonable decomposition into spin-orbit components split by 0.8 eV becomes possible (dashed line). Just as for Cs, the Rb edge is broadened more by Li additions than by Na. Miyahara *et al.*[13] report that the Rb edge remains sharp and shifts only by 0.04 eV at 26 at. % Rb in K, which is consistent with the same trends. A small but obtrusive extra feature is apparent near 15.2 eV in all four spectra. The same extra feature remains visible, although much reduced, in some of the spectra shown for Rb in Li. Its origin is not known.

3. *K in K-Li and K-Na*

Atomic K has its principal $3p^6 4s \rightarrow 3p^5 4s^2$ core excitations at[19] 18.71 eV ($P_{3/2}$) and 18.98 eV ($P_{1/2}$). In pure K,

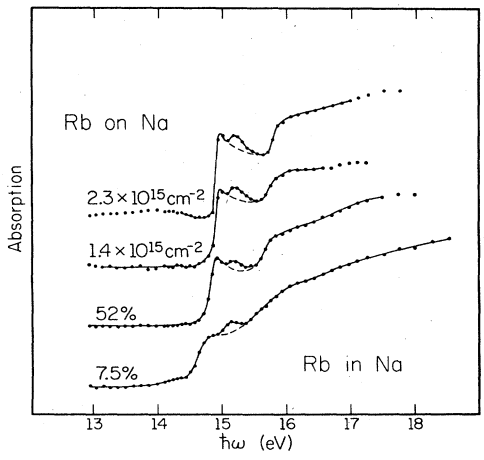

FIG. 7. Spectra of Rb in Rb-Na alloys of various compositions (at. %) scaled as in Fig. 4. The top two curves are spectra for coverages of about 3 and 5 monolayers of Rb on solid Na metal, to approximate the spectrum of pure Rb (see Fig. 1). The dashed lines interpolate under a weak but persistent feature of uncertain origin, but related to surface spectra (see paper II).

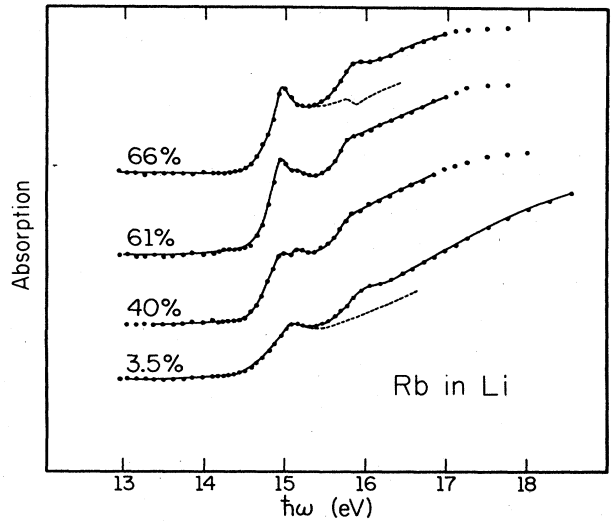

FIG. 8. Spectra of Rb in Rb-Li alloys of various compositions (at. %) scaled as in Fig. 4. Dashed lines indicate spin-orbit decompositions in a case where it is smooth (3.5 at. %) and where it is not smooth (66 at. %).

the sharply cusped M_3 edge is reported to occur at 18.2 eV with a width of about 60 meV. This is consistent with results of the present investigation of K in Li and in Na, which are collected in Fig. 9. Unlike the case for Cs and Rb, the K profile can be separated clearly into smooth spin-orbit partners even in the pure metal (dashed lines in Fig. 9). The top curve, obtained from a sample of

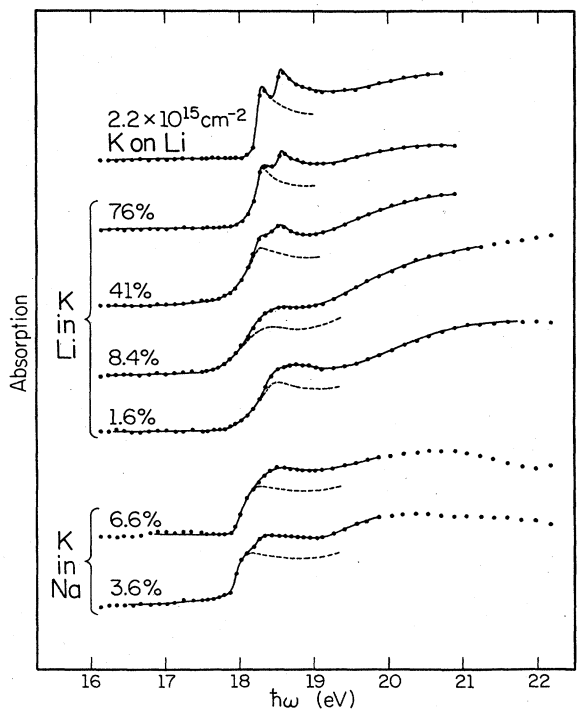

FIG. 9. Spectra of K in K-Li and K-Na alloys of various compositions (at. %) scaled as in Fig. 4. The top curve is for about 4 monolayers of K on Li metal, to approximate the spectrum of pure K. Dashed lines indicate spin-orbit decomposition, which is smooth in all cases for K core excitations.

2.2×10^{15} cm^{-2} or about 4 monolayers, exhibits all these features very clearly.

When Li is added the K edge broadens with a long Lorentzian-like tail extending to lower energies and the cusp on the $P_{3/2}$ spin-orbit component remains sharp but loses prominence. Between 40 and 10 at. % Rb the peak becomes rounded and the threshold remains extended; little difference is apparent between 8.4 at. % Rb and the dilute limit at 1.6 at. %. Smooth spin-orbit separation is possible throughout.

For K in Na we investigated only the dilute limit at 6.6 and 3.6 at. % K. There, the profile separates into spin-orbit partners smoothly, with each partner only $\sim$150 meV wide. This is much broader than the pure K edges, but rather minor when compared to other effects reported above. Similarly, the threshold red shift of about 0.25 eV is quite small. In other work Miyahara *et al.*[13] report that the M_3 edge of K remains sensibly unbroadened in K-Rb and K-Cs alloys, and is slightly blue-shifted.

4. Systematics

Certain correlations exist among the spectral profiles these diverse systems exhibit. We now summarize the experimental findings before turning to their interpretation in Sec. IV. There are three main points to be made.

First, for any given core, the broadening effect of the host lattice generally increases through the host sequence Cs, Rb, K, Na, Li; the degree to which core lines are broadened appears to increase through the core sequence [Li, Na] K, Rb, Cs; and these relationships occur in such a way that no core is substantially broadened in its own host lattice.

Second, the core profiles appear to broaden through a similar series of line shapes in each case. Thus, for Cs in Li and Na, Rb in Li and Na, and K in Li, an initial broadening having a Lorentzian tail is clearly evident. For Cs in Li and Na, and for Rb and K in Li, an intermediate regime is observed where the long tail disappears. Only for Cs in Li and Na is the linearlike regime attained.

The third and final correlation concerns the spin-orbit splitting. For Cs and Rb, with large splittings, a smooth spin-orbit decomposition is possible only when the profile is substantially broadened. However, the smaller splitting of K apparently leads to smooth spin-orbit superposition even for the sharp edge of the pure metal.

IV. DISCUSSION

The results presented in Sec. III show that a wide variety of threshold behavior occurs even in the simplest two-component systems, namely the alkali-alkali alloys, which have just one electron per cell and presumably rather isotropic conduction-electron properties. It is important to recognize that the new results are consistent with all previously established results. The $p^6s\rightarrow p^5s^2$ outer-core transitions of the pure alkali metals do indeed exhibit sharp, cusped threshold profiles; the cusps weaken, but the thresholds remain sharp in alloys among the three heavy alkali metals, just as reported by Miyahara *et al.*[13] It is nevertheless apparent that the earlier investigations missed a whole domain of threshold behavior. Experimentally, this occurs when excitations of heavy alkali-metal cores take place in light-alkali-metal hosts. Another feature of considerable interest is that the alkali-metal results link the cusped threshold behavior (e.g., Cs* in Cs) with the linear profile (e.g., Cs* in Li), which has zero absorption at threshold, by a smooth and systematic series of intermediate profiles. The linear profile has been reported for rare-gas impurities[10] and adsorbates[30] coupled to alkali metals, but a connection with the cusped behavior was previously lacking.

From a theoretical standpoint the MND formulation of the electronic excitation profile[6] does not appear to admit the possibility of such a striking evolution of response characteristics. The predictions depend solely on scattered phase shifts at the Fermi level, which surely cannot change so much in a simple monovalent alloy. The possibility therefore arises that the theory is partly or wholly incorrect. In what follows in Sec. IV A we examine several alternative mechanisms which might conceivably cause the observed effects. An intrinsic electronic mechanism appears to be the probable cause. This leads in Sec. IV B to a consideration of electronic structure in these alloys, and hence to universal scaling relationships which attempt to systematize the empirical correlations described in Sec. III B.

A. Possible broadening mechanisms

The broadening could possibly be attributed to inhomogeneity, to lattice response in the form of vibrational broadening, or to electronic response including lifetime broadening. These are considered successively in what follows.

1. Inhomogeneity

In random binary alloys, atoms of each species occur in a variety of near-neighboring environments. It is possible that the threshold behavior of any atom depends on its particular environment. In the alloy, therefore, the optical response is broadened by superposition of many differing responses, each with its own threshold characteristics.

To see whether this is a reasonable explanation of the observed behavior, we use a simple model in an attempt to reproduce the characteristics of Cs in Li. We use nearest-neighboring interactions only and assume that each atom has N equivalent neighbors. Then the probability in an alloy of concentration c that any atom has n like neighbors is

$$P_n(c)=\frac{N!c^n(1-c)^{N-n}}{n!(N-n)!}\ .$$

Figure 10 shows for an assumed $N=10$ nearest neighbors how $P_n(c)$ varies with n for $c=0.05$, 0.5, and 0.9. Under the reasonable supposition that, to a good approximation, each near neighbor merely displaces the spectrum by a given shift, the histograms in Fig. 10 indicate the expected broadening directly. An idea of the energy scale for the Cs-Li system is set by the fact that 10 Li neighbors redshift the threshold by about 0.4 eV.

It is apparent from Fig. 10 that this broadening mechanism is poorly suited to an explanation of the Cs*-Li spec-

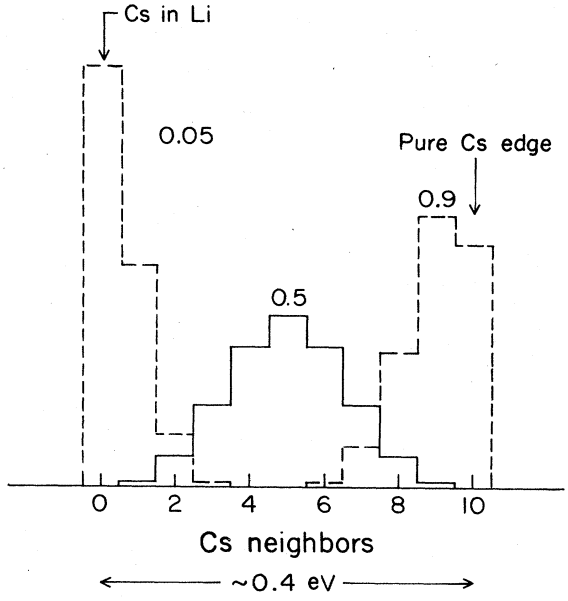

FIG. 10. Histograms showing broadening which occurs in a simple model of alloy inhomogeneity for fractional compositions of 0.05, 0.5, and 0.9 (see text). The observed broadening in the alloys has a quite different behavior (see, e.g., CsLi, Fig. 6).

tra. There are three qualitative problems. First, simple models of inhomogeneous broadening give the largest effects near intermediate compositions. In contradiction, the actual Cs response continues to broaden systematically from the lowest to the highest Li concentrations, reaching its largest width in the dilute limit when each Cs is homogeneously surrounded by Li atoms. Second, the inhomogeneous broadening provides no mechanism for the long Lorentzian tail introduced by relatively small Li additions. Finally, inhomogeneous broadening alone can never explain a linear, red-shifted profile in the dilute limit because the histogram tail extends to *higher* energy (Fig. 10); its convolution with a cusped intrinsic curve, like that for the pure metal, would then always be cusped.

While complicated models might be constructed to avoid these difficulties, no reasonable possibility appears to remain that the observed systematic broadening in several alloy systems arises from inhomogeneity alone. This mechanism is not pursued further in what follows.

2. *Phonon broadening*

The ground and core-excited configurations of atoms couple differently to the lattice. A well-known vibrational broadening of excitation profiles results from these effects.[31,21] It is possible in principle that the observed threshold broadening in alkali-metal alloys arises from this mechanism.

At least two compelling arguments make this proposed explanation highly improbable: both are quantitative. Phonon broadenings comparable to that displayed by Cs* at dilution in Li have been observed in metals only for halogen charge-transfer excitations[11] which involve impurity ionization and therefore cause a major change of coupling between the excitation center and the lattice. No such change of coupling appears at all likely for Cs. Were such an effect to exist, however, it would cause a large Stokes shift of the excitation.[31] The observed broadening for Cs* at dilution in Li corresponds to a width of 20—30 phonons of the Li lattice, with a Debye temperature of about 350 K. In the linear coupling approximation, the Stokes shift associated with this coupling would then be ~ 100 phonons or several eV. This Stokes shift would appear directly as a blue shift of the excitation threshold. Of course, Fig. 4 shows no sign of any blue shift within 1 order of magnitude of the predicted size. Rather, the observed threshold agrees rather well with the red shift predicted by the $Z+1$ model (Sec. II B). One must conclude that the profiles cannot arise from vibrational broadening alone.

3. *Electronic mechanism*

In the absence of inhomogeneous broadening it is possible to identify three intrinsic electronic mechanisms by which the optical response may be modified. There are lifetime-related processes, electron-hole—pair creation, and cooperative susceptibility effects. We consider each successively.

Core lifetimes in metals are normally determined by decay into conduction-band excitations; fluorescence from direct core-recombination processes also remains visible.[32] The decay is exponential by either mechanism, and the line broadening is consequently Lorentzian, unless interference occurs in the excited state. This latter complication most commonly involves a coupling between local and propagating excitations which are both optically active.[33] Lifetime effects cannot be eliminated as a possible mechanism of broadening. It is an attractive means by which the sharp threshold edges of pure metals could develop the extended Lorentzian tails observed in some of the alloys studied here. An order-of-magnitude or more decrease of excited-state lifetime seems to be required to explain the observed line shapes. No underlying mechanism for a change of this nature has been proposed to date.

Electron-hole—pair creation is the mechanism by which core line shapes are determined in the MND theory,[6] and it is undoubtedly the main effect by which the core lines are spread into shoulders. In simple terms it is occasionally considered that the sharp thresholds arise because the core electron can be excited into any of the continuum of unoccupied states that lie above a sharply defined Fermi level; in general, however, this is not a correct description. Instead, one should consider a relaxed, self-consistent excited configuration in which quasiparticle pairs are, in addition, generated by the optical event. The profile above threshold then reflects the matrix elements for transitions to various excitation levels of the electron liquid. It is an experimental fact that in some cases optical absorption begins with an abrupt step at threshold (e.g., the pure alkali metals) and that in other cases the absorption is zero at the threshold and rises thereafter in an approximately linear ramp (e.g., rare-gas impurities, Cs in Li and Na, Cs on Mg). No comprehensive theory is yet available to con-

nect these various observations with the quasiparticle pair-creation mechanism, but the phenomena clearly extend over an energy range with which this mechanism is compatible.

A third process which may possibly modify excitation line shapes in solids is the interaction among neighboring excitation centers. Each core, in effect, produces a local field at other core locations, and a cooperative modification of all the excitation amplitudes can ensue. The mechanism has been discussed by Nagel and Witten.[34] Since quite sharp threshold steps are observed for impurities at dilution in some systems (e.g., Cs* in K, Fig. 6), it is not possible that they originate only in local-field effects. These effects may nevertheless possibly contribute to the sharpness of the anomalies observed near some sharp threshold edges.

B. Bound states and scaling

The preceding discussion identifies the probable origins of the observed core line shapes in electronic processes including lifetimes, electron-hole—pair creation, and, possibly, internal fields. It does not resolve the causes of the observed line-shape transitions, or, for that matter, the significance of the limiting line shapes. These are the questions we now examine.

It seems likely that the core line shapes are determined by bound-state formation. The reasons for this assertion are made clear by Fig. 3, which shows the excited s^2 levels of alkali-metal atoms relative to the host band states. Only for Cs* in Li and Na and for Rb* in Li do the s^2 levels of the core-excited atom lie above the band average energy. These are precisely the three cases where the experiments find the largest broadening of the core threshold. K* in Li and Na, and Rb* in Na, are marginal cases, according to Fig. 3, in which the excited s^2 levels lie at or just below the band average. The experiments show substantial broadening for N* in Rb and some smaller broadening for K* in Li and Na. In all other cases the s^2 valence orbitals of the excited atom lie at or below the host conduction-band bottom in Fig. 3. These are all systems in which the abrupt core-excitation edges are observed to remain relatively unbroadened.

We see that the excited-state chemical structure explains the experimental correlation of core broadening with host species quite accurately. Sharp thresholds with cusps correspond to bound excited states. This effect appears to be related to the emergence of "white-line" structure at threshold on x-ray transitions which have localized final states. The opposite limit, in which the line shape resembles a linear ramp, occurs when the excited orbitals are fully mixed into the conduction band, at or above the band center. This result again appears related to other earlier results. The excited levels of rare-gas atoms resemble alkali-metal-atom ground states, and therefore also mix strongly with alkali-metal band states (this is made obvious by the $Z+1$ model). It is known from earlier work[10] that rare-gas core excitations in alkali metals exhibit linear profiles with zero absorption at threshold similar to that for Cs in Li. Thus, a comprehensive experimental view of these diverse systems appears to be emerging.

Note, however, that a significant problem remains for the theory. The sharp thresholds with cusps, which have been the main examples of the MND "x-ray-edge anomaly," may relate instead to the white-line phenomena of localized state formation. Linear threshold profiles, which find no explanation in MND theory, appear to be the normal response of the conduction-electron liquid to a strongly coupled optical shock.

Similarities of detail among the line shapes in Figs. 4—9 encourage a more quantitative approach to the analysis of these data. Figure 11 shows all the threshold data arranged on a single figure with each column an alloy system and with position in the column representing the shape. The Cs*-Li system provides the widest spectrum of line shapes, and these are arranged according to actual composition. In the columns for other alloy systems the spectra are placed at the level where they best fit the sequence of Cs*-Li profiles. On the whole this can be done fairly satisfactorily, although the available experimental precision is not sufficient to establish how closely the data conform to a truly universal set of profiles. Figure 11 provides an "effective Cs*-Li concentration," c, which specifies the position of each line shape within the Cs*-Li sequence. In the absence of a line-shape theory we can use this parameter to determine the way line shapes depend on other properties of the various alloy systems. As a practical matter in what follows, all sharp lines with a threshold step less than 100 meV wide were assigned $c=100$, since they lie within a factor 2 of the limit of use-

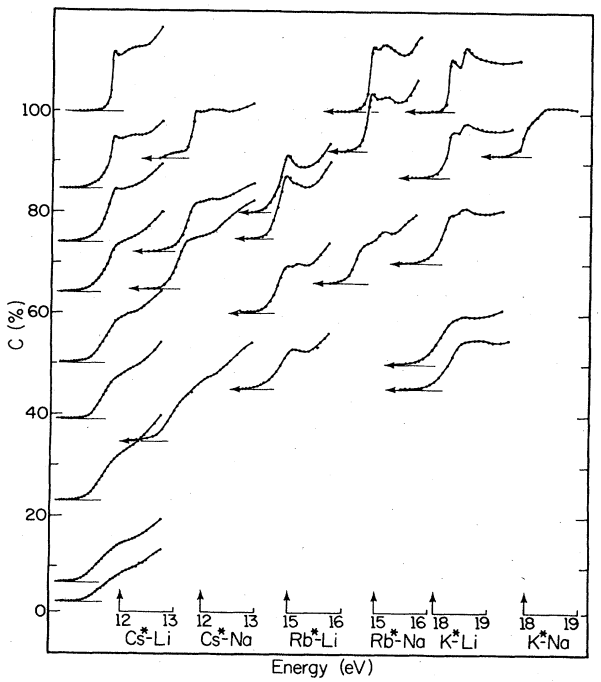

FIG. 11. Outer-core spectra of alkali-metal atoms in the alkali-alkali alloys indicated (at. %). The left-hand column shows Cs in Li metal, with spectra placed at heights proportional to the composition. For the remaining systems the spectra are placed at those heights at which the line shapes fit appropriately among the Cs-Li data. This identifies an "effective composition" c for the edge profile in each alloy.

ful experimental resolution.

We now require a measure of the excited-state structure relevant to the correlations obtained above. The splitting

$$\Delta = E_i - \bar{E}$$

between the band average binding energy $\bar{E}$ and the s^2 binding energy E_i of the levels of the excited impurity is one important quantity (these energies are shown in the inset sketch in Fig. 12). Therefore the parameter

$$\xi = \Delta / E_F$$

suggests itself as a suitably scaled dimensionless measure of excited-state structure by which questions of universality in the response may be investigated. In effect, ξ is the ratio of the local perturbation to the conduction-electron kinetic energy. It affords a concise but comprehensive scaled description of the excited configuration.

A plot of ξ against c for all the alloy spectra reported here, all the pure metals, and all the results of Miyahara *et al.*[13] is displayed in Fig. 12. All the points scatter fairly closely about a common line. This indicates that the universal scaling description has at least a semiquantitative validity. An important point is that c departs from 100 approximately at $\xi = 0.6$, which means $E_i - \bar{E} = 0.6 E_F$. For a parabolic band this is exactly the condition at which the s^2 levels enter the bottom of the conduction band. Note that the behavior there is quite smooth. This is in accordance with the demonstration by Kohn and Majumdar[35] that no abrupt changes of physical properties accompany bound-state formation, even in one-electron theory.

In practice, Δ and E_F for the values of ξ in Fig. 12 were obtained by the simplest useful prescriptions. Thus the Fermi energy is

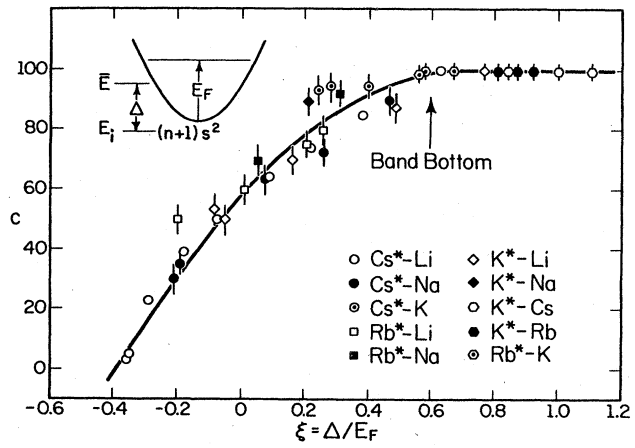

FIG. 12. Graph showing core line shape, specified by the effective composition c (see Fig. 11 and text), as a function of the parameter $\xi = \Delta / E_F$, which specifies the electronic structure of the excited configuration (see inset at upper left) for alkali-metal alloys. Hexagonal symbols indicate data of Miyahar *et al.* (Ref. 13). The data fall close to a specific variation of ξ with c, which indicates that the electronic structure determines the universal sequence of line shapes. It appears that the width starts to increase significantly near $\xi = 0.6$, which is precisely when the s^2 levels are degenerate with the band bottom (see inset).

$$E_F^{-3/2} = c_1 E_{F1}^{-3/2} + (1 - c_1) E_{F2}^{-3/2} ,$$

which follows when Vegard's approximation is used to obtain the alloy volume. Here, E_{F1} and E_{F2} are the Fermi energies of the two pure metals and c_1 is the actual concentration of metal 1. The correlations appear to work out best for "measured" rather than free-electron values of E_F, so these[36] were used in the results of Fig. 12. Similarly, the mean band energy is

$$\bar{E} = c_1 (I_1 + E_{c1}) + (1 - c_1)(I_2 + E_{c2}) ,$$

where I_1 and I_2 are atomic ionization energies and E_{c1} and E_{c2} are cohesive energies of the two pure metals. The energies of intersolution are thereby assumed to be zero (see Sec. II). Finally, the energy E_i with which the band average is compared is obtained from

$$E_i = I^* + E_c .$$

This assumes that the excited s^2 levels maintain the same splitting from the ground s level as in the free atom.

The real inhomogeneous alloy is a good deal more complicated than this simple model. We reiterate (Sec. II) that the electronic structures determined from comprehensive calculations may possibly differ in detail from those deduced here. Also, it is hard to be certain that the correlation in Fig. 12 has a unique interpretation because most energies in the alkali-metal systems vary systematically with volume. These uncertainties may have less consequence for the validity of the scaling ideas, however. To the degree that the parameter ξ employed here correctly describes the *driving forces* which determine the electronic structure, the general conclusions drawn from Fig. 12 remain unaffected. Only the value of ξ which corresponds to the band bottom might fall into question. In reality, however, this occurs in the region of sharp thresholds ($c = 100$) associated with rather homogeneous alloys, so that this result, also, probably retains a considerable degree of validity.

C. Concluding comments

The phenomena investigated in this paper occur within an energy range of ~ 500 meV, and variations of response over 100 meV are important. Resolution on the order of 50 meV or better is desirable to explore these processes adequately. The present work hardly meets these requirements, owing to the available time and signal to noise. Many of the spectra in the existing literature involve worse resolution, particularly for x-ray-photoemission spectroscopy (XPS) results[8] where the resolution may be an order of magnitude worse than that required. Only for the alkali metals, and Mg and Al, do the natural widths of outer-core-excitation edges appear to permit such resolution in the first place. Of these, it must be stated that the $L_{2,3}$ edge of the metal Al is so similar to that of its neighbor Si,[37] a nonmetal with a band gap of 1 eV, that their explanations, also, might reasonably be similar; this appears to eliminate a substantial Fermi-liquid involvement. Mg is not a suitably simple metal. Its behavior is complicated by the details of its band structure;[38] excitonic phenomena occur in its conduction band,[39,18] and a number

of striking and unexplained effects are seen in the core spectra of Mg-based alloys.[40] Consequently, the alkali $np^6(n+1) \rightarrow np^5(n+1)s^2$ excitations have been the main experimental testing ground of "simple" x-ray-edge behavior.

In the present paper we report results which indicate that the previous physical understanding of the alkali-metal excitation edges may be mistaken. We have shown that the sharp alkali-metal edge and "x-ray-edge anomaly" occurs in the presence of a marked tendency to bound-state formation, and is otherwise absent. Threshold-energy calculation in Sec. II indicate that the observed edges occurs within perhaps 0.2 eV of the predicted thresholds. Therefore they may well be, in fact, the true thresholds rather than shakeoffs occurring some distance above fully suppressed thresholds. The same type of peaked phenomenon in molecules and solids, with sharp edges having a strongly peaked threshold structure (white lines), has been recognized for many years as arising from just such a localization of the excited state.[14] It appears that the alkali-metal threshold behavior has a similar origin. Additional evidence presented in paper II suggests that neighboring like cores may possibly contribute to the emergence of sharp structure. A final assessment of the degree to which the s^2 levels actually localize, and the extent to which core-core interactions, either electronic or electromagnetic, modify the sharp structure, must await future detailed calculations. However, the fact that the sharp structure is associated with these general causes appears to be securely established.

Only in the cases of Cs*-Li and Cs*-Na is the limiting behavior of an approximately linear threshold line shape reached; the remainder appear to possess intermediate responses. For Cs*-Li the identification is aided by good agreement with the predicted red shift (Sec. II) of the threshold from that in pure Cs. Figure 3 makes clear why other examples of linear profiles are unlikely to be found in these systems, except perhaps at high pressure, where the conduction bands broaden. One infers that the linear profile is the electron liquid response to a strongly coupled optical shock. If so, no theory is at present available to describe this behavior. We note elsewhere, however, that the density of available single-quasiparticle—pair states varies linearly with their energy in a Fermi liquid. One possibility is that the local shock projects the conduction-electron system with equal probabilities into any of the low-lying states which contain a single electron-hole pair.[15]

If the theory predicts incorrect results it is natural to inquire as to what is wrong with the theory. In the case of the x-ray edge the answer is not known in detail at present. This is one of an important class of problems in which the behavior necessarily blends Fermi-liquid properties with local chemical phenomena. The excited states are, after all, long-lived configurations of a conduction-electron liquid in which one locality having atomic dimensions is strongly deformed. It is not possible at present to calculate the matrix elements of local operators in an interacting Fermi liquid. In MND-type theories the behavior is simulated by determinantal approximations, with the matrix elements parametrized. Such approximations may be particularly poor for the alkali metals, in which Coulomb correlations are strong. In any event, the regime of behavior is one in which a number of quasiparticle pairs are predicted to be created by the local event. This requires that quasiparticles overlap strongly in and near the central cell at the moment after the shock, so that the Landau theory of Fermi liquids is not necessarily applicable. It is apparent that the core-excitation processes investigated here may provide an opportunity to explore new regimes of Fermi-liquid behavior which are otherwise inaccessible.

V. SUMMARY

In the present work we show how to estimate core-excitation energies and core-excited electronic structures in alkali-alkali alloys. Core-excitation profiles in a variety of these alloys have been investigated experimentally, using differential reflectance methods on samples quench-condensed at liquid-He temperature. The observed threshold profiles exhibit a range of shapes extending from sharp shoulders with cusped threshold peaks to linearlike behavior above a fully suppressed threshold. All these data, and results in the literature for pure alkali metals and alkali-alkali alloys, can be arranged in an approximately universal sequence of line shapes and ordered by a single scaling parameter, ξ. This parameter is just the splitting of the excited s^2 levels below the band center, scaled by the Fermi energy. It is deduced that the linear profile corresponds to excited orbitals which fully mix into the middle of the band or above. The cusped "x-ray-edge" profiles are associated with bound-state formation, and are presumably related to "white-line" phenomena. Our conclusions differ markedly from earlier interpretations of core-excitation spectra. Quantitatively accurate theories are not currently available to discuss either limit of the line-shape behavior.

ACKNOWLEDGMENTS

This research was supported by the National Science Foundation under Grant No. DMR-80-08139. We thank the staff of the University of Wisconsin Synchrotron Radiation Center at Stoughton for help during the experiments. Use of machine shop and computational facilities supported by the National Science Foundation—Materials Research Laboratories Program Grant No. DMR-83-16981 at the University of Illinois is acknowledged.

*Permanent address: AT&T Bell Laboratories, Crawfords Corner Road, Holmdel, NJ 07733.

†Permanent address: Department of Physics, Brookhaven National Laboratory, Upton, NY 11973.

[1]T. Ishii, Y. Sakisaka, and S. Yamaguchi, J. Phys. Soc. Jpn. **42**, 876 (1977).

[2]P. W. Anderson, Phys. Rev. Lett. **18**, 1049 (1967).

[3]G. D. Mahan, in *Solid State Physics*, edited by F. Seitz and D. Turnbull (Academic, New York, 1974), Vol. 29.

[4]P. Nozières and C. T. de Dominicis, Phys. Rev. **178**, 1079

(1969).
[5]S. Doniach and M. Sŭnjić, J. Phys. C **3**, 285 (1970).
[6]J. Wilkins, in *X-Ray and Inner Shell Physics,* edited by B. Crasemann (AIP, New York, 1982).
[7]P. H. Citrin, G. K. Wertheim, and M. Schlüter, Phys. Rev. B **20**, 3067 (1979).
[8]See S. E. Schnatterly, in *Solid State Physics,* edited by F. Seitz and D. Turnbull (Academic, New York, 1979), Vol. 34, for electron scattering and P. H. Citrin, G. Wertheim, and Y. Baer, Phys. Rev. B **16**, 4256 (1977) for XPS.
[9]C. Kunz, H. Peterson, and D. W. Lynch, Phys. Rev. Lett. **33**, 1556 (1974); J. J. Ritsko, S. E. Schnatterly, and P. C. Gibbons, Phys. Rev. B **10**, 5017 (1974); L. Hedin, J. Phys. (Paris) Colloq. **39**, C4-103 (1978).
[10]D. J. Phelps, R. A. Tilton, and C. P. Flynn, Phys. Rev. B **14**, 5254 (1976).
[11]R. Avci and C. P. Flynn, Phys. Rev. B **19**, 5981 (1979).
[12]These results are reviewed by C. P. Flynn, Surf. Sci. (to be published).
[13]T. Miyahara, S. Sato, H. Hanyu, A. Kakizaki, S. Yamaguchi, and T. Ishii, J. Phys. Soc. Jpn. **49**, 194 (1980).
[14]See, e.g., L. V. Azaroff and D. M. Pease, in *X-Ray Spectroscopy,* edited by L. V. Azaroff (McGraw-Hill, New York, 1974).
[15]T.-H. Chiu, D. Gibbs, J. E. Cunningham, and C. P. Flynn, J. Phys. F **13**, L23 (1983); Phys. Rev. Lett. **49**, 815 (1982).
[16]D. Gibbs, T.-H. Chiu, J. E. Cunningham, and C. P. Flynn, following paper, Phys. Rev. B **32**, 602 (1985).
[17]See, e.g., Ref. 10; also, for noble metals, C. P. Flynn, J. Phys. F **10**, L315 (1980) and, for transition metals, B. Johansson and N. Martensson, Phys. Rev. B **21**, 4427 (1980).
[18]J. C. Boisvert, P. W. Goalwin, A. B. Kunz, M. H. Bakshi, and C. P. Flynn, Phys. Rev. B **31**, 4984 (1985).
[19]C. E. Moore, *Atomic Energy Levels,* (U.S. GPO, Washington, D.C., 1971).
[20]For cohesive energies, see K. A. Gschneider, in *Solid State Physics,* edited by F. Seitz and D. Turnbull (Academic, New York, 1964), Vol 16; E. P. Wigner and F. Seitz, in *Solid State Physics,* edited by F. Seitz and D. Turnbull (Academic, New York, 1955), Vol. 1
[21]C. P. Flynn, Phys. Rev. Lett. **37**, 1445 (1976).
[22]H. K. Wolff, K. Radler, B. Sonntag, and R. Haensel, Z. Phys. **257**, 353 (1972).
[23]R. Haensel, G. Keitel, B. Sonntag, C. Kunz, and P. Schreiber, Phys. Status. Solidi A **2**, 85 (1970).
[24]Unless otherwise indicated, solubilities quoted in this paper are taken from alloy data reports in the following standard sources on *Constitution of Binary Alloys,* edited by M. Hansen and K. Anderco (McGraw-Hill, New York, 1958); first supplement, edited by R. P. Elliott (1965); second supplement, edited by F. A. Shunk (1969).
[25]T. Yokokawa and O. Kleppa, J. Chem. Phys. **40**, 46 (1964).
[26]N. F. Mott, J. Phys. Radium **23**, 594 (1962).
[27]J. E. Inglesfield, J. Phys. F **2**, 878 (1972).
[28]See, e.g., J. C. Boisvert, Ph.D. thesis, University of Illinois, 1984 (unpublished).
[29]J. E. Cunningham, D. K. Greenlaw, and C. P. Flynn, Phys. Rev. B **22**, 717 (1980).
[30]D. Gibbs, J. E. Cunningham, and C. P. Flynn, Phys. Rev. B **22**, 5292 (1984).
[31]A. M. Stoneham, *Theory of Defects in Solids* (Oxford University Press, Oxford, 1974).
[32]H. W. B. Skinner, Philos. Trans. R. Soc. London, Ser. A **239**, 95 (1946); T. Kobayashi and A. Morita, J. Phys. Soc. Jpn. **28**, 457 (1970); see also articles collected in Jpn. J. Appl. Phys. **17**, Suppl. 17-2 (1978).
[33]U. Fano, Phys. Rev. **124**, 1866 (1961).
[34]S. R. Nagel and T. A. Witten, Phys. Rev. B **11**, 1623 (1975).
[35]W. Kohn and C. Majumdar, Phys. Rev. **138**, A1677 (1965).
[36]D. J. Fabian, L. M. Watson, and C. A. W. Marshall, Rep. Prog. Phys. **34**, 601 (1971); A. H. Wilson, *Theory of Metals* (Cambridge University Press, Cambridge, 1936).
[37]Data for Al are discussed in Refs. 7 and 8; for Si, see F. C. Brown, R. Z. Bachrach, and M. Sibowski, Phys. Rev. B **15**, 4781 (1977).
[38]R. P. Gupta and A. J. Freeman, Phys. Rev. Lett **36**, 1194 (1976).
[39]M. H. Bakshi, G. A. Denton, A. B. Kunz, and C. P. Flynn, J. Phys. F **12**, L235 (1982); M. H. Bakshi, G. A. Denton, C. P. Flynn, J. C. Boisvert, and A. B. Kunz, Phys. Rev. B **31**, 4972 (1985).
[40]A number of results are discussed in D. J. Sellmyer, in *Solid State Physics,* edited by F. Seitz and D. Turnbull (Academic, New York, 1977), Vol. 33.